Performance Evaluation of Finite Elements for Analysis of Advanced Hybrid Laminates

Hemanth R. H, Ruchin P, Gourav G, Venkatesha K. S and Ravi Kumar, G. V. V

Infosys Technologies Limited, Electronic City, Hosur Road, Bangalore, India

Henry Sklyut, Michael Kulak and Markus Heinimann

Alcoa Technical Center, 100 Technical Drive, PA 15069, United States

Abstract: Advanced hybrid laminates (AHL) are based on advanced metal alloys and involve the strategic placement of Fiber Metal Laminates (FML) and/or fiber prepreg only where necessary to enhance structural performance. These hybrid structural concepts bring best of both metals and composites. Finite element analysis of these layered structures is quite complex involving simulation of interaction between metallic and composite layers, accurate prediction of in-plane and out-of-plane stresses, contact simulation and progressive failure analysis of metallic and composite layers. The finite element chosen should be able to accurately predict both in plane and out of plane stresses. This paper presents a study of isotropic, orthotropic, composite and hybrid structures under tension, bending, shear and combined loadings using various 2D and 3D finite elements and their accuracy in predicting stresses. Abaqus is chosen for its strong nonlinear and contact analysis capabilities and provisions to write user subroutines for performing failure analysis of hybrid laminates. Available analytical results have been used to evaluate the performance of finite elements. Based on the detailed study, 3D solid element C3D20 is recommended for accurate analysis of AHL. A typical aircraft wing bottom skin hybrid stiffened panel has been analyzed using global local analysis to predict the local stresses using C3D20 solid elements. The results are analyzed from aircraft designer perspective.

Key Words – Advanced Hybrid Laminates, FEM, Element Evaluation and Abaqus

Notations

E	Young's Modulus of isotropic material
ν	Poisson's Ratio of isotropic material
E_L, E_T, E_Z	Young's Moduli in three major directions of a ply
ν_{LT}, ν_{LZ}, ν_{ZT}	Poisson's Ratios of a ply
G_{LT}, G_{LZ}, G_{ZT}	Shear Moduli of a ply
x ,y, z	Coordinate axes
u, v, w	Displacements along x, y, z axes
θ_x, θ_y, θ_z	Rotations about x, y, z axes

σ_{xx}, σ_{yy}, σ_{zz}	Normal stresses in x, y, z directions respectively
σ_{xy}, σ_{yz}, σ_{xz}	Shear stresses in xy, yz, zx planes respectively

1. Introduction

Advanced hybrid structures are based on advanced metals and involve strategic placement of fiber metal laminates and/or fiber prepreg only where necessary to enhance structural performance. Alcoa Technical Center (ATC) has developed many advanced hybrid structural concepts for aircraft structures (Kulak 2004, Heinimann, 2005, Heinimann, 2007, and Bucci, 2006) bringing together best characteristics, design practices and technologies of metals, composites and FMLs. Advanced hybrid structures allow tailoring of structural performance by varying metallic and fiber volume fractions, fiber orientations etc. Hybrid structural concepts will help in realizing thick laminates required for aircraft wing skins.

Analysis of hybrid laminates using classical laminated plate theories are applicable to simple configurations only. Finite element approach is most suitable for the analysis of hybrid laminates with multiple material systems and different orientations. Hybrid laminates with irregular boundaries and discontinuities like holes and cutouts can be easily modeled and analyzed through FEA. 2D shell elements use classical laminate plate theory and cannot predict out of plane stresses. Analytical approaches like integration of equilibrium equations can be used to compute out of plane stresses from in plane stresses (Ganapathy, 1998). Using solid elements, interlaminar stresses in hybrid laminates can be accurately computed. Finite element approach facilitates to take into account both material and geometric nonlinearities. Residual stresses can be easily computed to account for the curing effects. Progressive failure analysis along with multiple failure criteria and various material degradation models can be easily incorporated in finite element analysis framework. Based on these factors, thermo-mechanical analysis of advanced hybrid laminates with notches can be best performed using finite element approach. However, it is essential to use appropriate elements to simulate accurate behavior. Elements selected to perform finite element analysis should have the following characteristics:

- Able to capture both in-plane and out of plane stresses especially the interlaminar shear and normal stresses between metallic and composite layers
- Able to capture stress raisers in free edges and notched regions
- Accurately capture material non-linearity of metallic layers
- Allow modeling of progressive failure analysis of composite layers
- Amenable to implementation of material degradation models for accurate analysis of progressive failure
- Ability to compute residual thermal stresses and capture interaction of thermo-mechanical stresses
- Amenable to modeling and analysis involving contacts

Abaqus is chosen for its excellent nonlinear analysis and contact modeling capabilities. In order to select the best finite element, both 2D shell and 3D solid elements are studied. Sample test problems are identified such that out of plane load is predominant causing development of considerable out of plane stresses in the structure. Abaqus finite element analysis results are compared with available classical solution results and with results from NASTRAN. The performance of elements is evaluated on isotropic beams, isotropic/orthotropic plate, composite/hybrid laminates under various loading conditions like tension, bending, shear and combined loading.

2. Stress Analysis of cantilever beam

An isotropic cantilever beam subjected to end concentrated load is studied and the results are compared with the available analytical solution. The beam length, width and depth as shown in Figure 1 are taken as 150mm, 2.5mm and 5mm respectively.

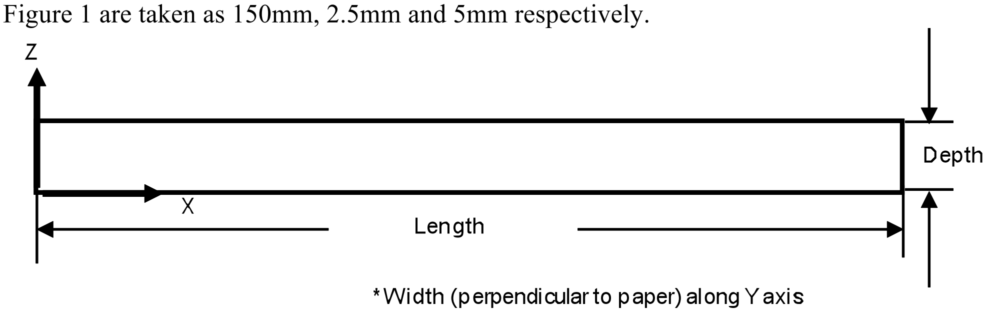

Figure 1. A typical beam along with dimensions and reference axis system

The beam is modeled using various Abaqus 3D elements namely linear fully integrated element (C3D8), linear reduced integrated element (C3D8R), quadratic fully integrated element (C3D20) and quadratic reduced integrated element (C3D20R). The material is Aluminum with E and ν as 70GPa and zero respectively. Poisson's ratio is taken as zero to compare analysis results with Euler-Bernoulli analytical solutions (James, 1984). The beam is analyzed for concentrated load 5N at the free end. The beam is modeled with 30 elements along the length, one element along the width and varied number of elements along the depth.

Transverse deflection in the direction of force at the free end and shear stress in direction of force acting on cross section plane at the constrained face are given in Table 1 along with the Euler – Bernoulli beam analytical solution (James, 1984).

Element Type	Number of elements through depth	Abaqus Results		Analytical Results	
		Tip Deflection (mm)	Transverse Shear stress (MPa)	Tip Deflection (mm)	Transverse Shear stress (MPa)
C3D8	1	2.996	33.211	3.0857	0.600
	2	2.189	25.488		
	4	2.088	24.357		
C3D8R	1	218.136	0.400		
	2	4.096	0.400		
	4	3.289	0.541		
C3D8R (Enhanced Hourglass control)	2	3.087	0.4		
	4	3.087	0.5497		
C3D20	1	3.087	0.582		
	2	3.088	0.598		
	4	3.088	0.612		
C3D20R	1	3.087	0.400		
	2	3.088	0.420		
	4	3.088	0.495		

Table 1. Results for cantilever beam analysis

As indicated, C3D8 elements did not predict accurate displacements even with more elements through the depth of the beam and had shear locking. In the literature, reduced integration elements are used to reduce the influence of shear locking. Abaqus results of C3D8R without enhanced hourglass control predict inconsistent results and it is difficult to judge accuracy of these results. However, with enhanced hourglass control, C3D8R is able to predict accurate results.

C3D20 elements predict results that are close to analytical solution. C3D20R elements predict displacement results that are close to that of C3D20 results. However stress results are inaccurate with the same mesh. Abaqus does not have enhanced hour glass control for C3D20R elements. Figure 2 shows the transverse stress distribution through the thickness at a typical cross section close to fixed edge obtained using C3D20 elements. There is difficulty in getting accurate distribution of transverse shear stress (zero at free surfaces and 0.6 at middle) at any cross-section of the beam. However distribution is close to what theory predicts..

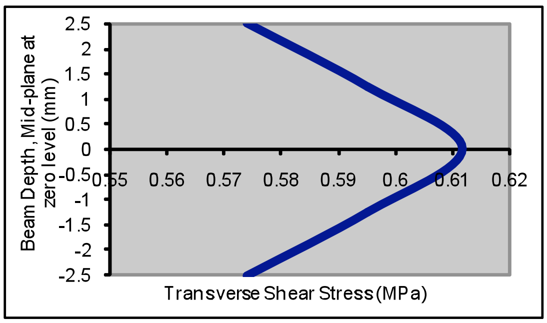

Figure 2. Transverse shear stress distribution

Table 2 shows the comparison of Abaqus and NASTRAN results for 8-noded brick elements and the two show similar trends. Abaqus also has special types of elements called incompatible elements (C3D8I) whose performance is better. However, these elements are sensitive to shape. The regular rectangular or square elements give very good performance and the irregular elements predict completely wrong stresses. The results for regular and irregular C3D8I elements are also shown in Table 2.

FE Tool	Element Type	Number of elements through depth	FE Analysis		Analytical	
			Tip Deflection (mm)	Transverse Shear Stress (MPa)	Tip Deflection (mm)	Transverse Shear Stress (MPa)
Abaqus	C3D8	1	2.996	33.211	3.087	0.600
	C3D8I (Square shape)		3.087	0.4		
	C3D8I (Irregular shape)		3.018	15.79		
NASTRAN	CHEXA8		2.058	0.400		
Abaqus	C3D8	4	2.088	24.357		
	C3D8I (Square shape)		3.087	0.567		
	C3D8I (Irregular shape)		3.041	9.949		
NASTRAN	CHEXA8		2.058	0.508		

Table 2. Comparison of Abaqus and NASTRAN results for cantilever beam

3. Bending of isotropic homogeneous plate under uniform pressure

A simply supported square steel plate subjected to a uniform pressure of 1 MPa on the top face is analyzed using Abaqus. X and Y axes are along the edges of the plate as shown in Figure 3.

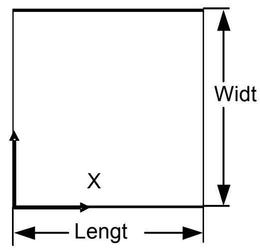

* Thickness (perpendicular to paper) along Z

Figure 3. Typical Plate along with dimensions and reference axis system

Plate has sides of 50mm and thickness of 1 mm and is modeled using S4, C3D8 and C3D20 elements. Plate material properties are E = 210 GPa and ν = 0.3. Number of elements through the plate thickness is varied. Finite element results are compared with classical plate theory (Timoshenko, 1959) results. Interlaminar stress components given in thesis (Ganapathy, 1998) are used to compare the current FE results.

Boundary conditions used in shell model (BC1) is: at edges x=0 & x=a the translational degrees (u, v, w) and rotational degrees (θ_x, θ_z) are restrained and at edges y=0 & y =b the translational degrees (u, v, w) and rotational degrees (θ_y, θ_z) are restrained. Boundary conditions used in solid model (BC2) is: all along the four edges the translational degree of freedom w is restrained.

Table 3 presents results of the analysis using S4 , C3D8 and C3D20. Even with only 1 element through the thickness, vertical deflections are in good agreement with the classical plate theory. C3D8 stress results are not accurate.

Element Type	Mesh Size	Aspect Ratio	Boundary Condition	Abaqus Results		Analytical Results	
				Central Vertical Deflection (mm)	Normal Stress $\sigma_{xx} = \sigma_{yy}$ (MPa)	Central Vertical Deflection (mm)	Normal stress $\sigma_{xx} = \sigma_{yy}$ (Mpa)
S4	40 x 40	1.25	BC1	1.323	At Center: 718 At Edge: 0	1.321	At Center 718.5 At Edge 0.0
C3D8	40x40 x2	2.5	BC2	1.174	At Center: 379 At Edge:24		
	40x40 x4	5		1.079	At Center: 470 At Edge: 29		
	40x40 x10	12.5		1.060	At Center: 530 At Edge: 30		

	80x80 x10	6.25		1.263	At Center: 629 At Edge: 18		
	160x160x10	3.125		1.329	At Center: 660 At Edge: 8		
C3D20	40x40 x1	1.25	BC2	1.342	At Center: 726 At Edge: 14		
	40x40 x2	2.5		1.344	At Center: 727 At Edge: 10		
	40x40 x4	5		1.344	At Center: 727 At Edge: 11		
C3D20R	40x40 x4	5	BC2	1.345	At Center: 728 At Edge: 6		

Table 3. Results of Simply supported plate analysis

Table 4 shows the comparison of Abaqus and NASTRAN results for the plate bending problem. Comparing the results of Tables 3 and 4, Abaqus C3D20 elements are clearly more accurate.

Element Type	Mesh Size	Aspect Ratio	Boundary Condition	FEA Results		Analytical Results	
				Central Vertical Deflection (mm)	Normal Stress $\sigma_{xx} = \sigma_{yy}$ (Mpa)	Central Vertical Deflection (mm)	Normal stress $\sigma_{xx} = \sigma_{yy}$ (MPa)
HEXA8 (NASTRAN)	40x40 x10	12.5	BC2	1.049	At Center: 517 At Edge: 27	1.321	At Center 718.5 At Edge 0.0
C3D8 (Abaqus)				1.050	At Center: 530 At Edge: 30		
C3D8I (Abaqus)				1.337	At Center: 724 At Edge: 45		

Table 4. Comparison of Abaqus and NASTRAN elements results

Out of plane shear stresses (σ_{xz}, σ_{yz}) obtained from FEA on plate modeled with C3D20 elements are shown in Figure 4. These predictions are similar to the results obtained by Ganapathy (1998). In FEA, the peak stress σ_{xz} (at x=0 and y=25) is obtained as 42MPa which is higher than the actual stress level (25MPa from analytical solution) as these points are near to the supports. But high stress zone is limited to 3.75 mm from the supported edge in FEA beyond which FE solution is in close agreement with the analytical solution. Variation of σ_{xz} through the thickness near and away from the supported edge is shown in Figure 5.

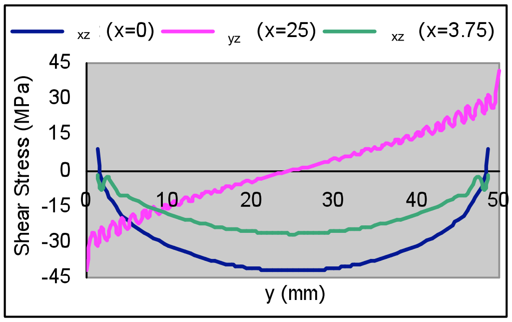

Figure 4. Variation of σ_{xz} and σ_{yz} along y

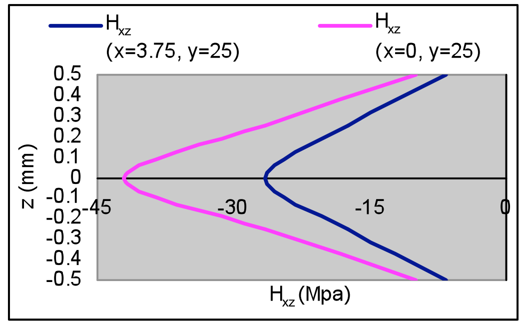

Figure 5. variation of σ_{xz} through the thickness

4. Bending of orthotropic plates under uniform pressure

An orthotropic square plate, with sides of 20mm and thickness of 2.8 mm, simply supported on all edges was analyzed under uniform lateral pressure of 1MPa at the top. All the dimensions and axis system of the plate configurations are same as in Figure 3. These configurations are analyzed using C3D20 elements. Following boundary conditions are used:

along the edges x=0 and x=a, v=0 and w=0; along the edges y=0 and y=b, u=0 and w=0

The orthotropic material properties used in the analysis are

E_L = 210000 MPa, E_T = 110250.420 MPa, E_Z = 119574.042 MPa, G_{LT} = 61490.753 MPa, G_{LZ} = 37398.527 MPa, G_{TZ} = 62397.921 MPa, ν_{LT} = 0.4405, ν_{LZ} = 0.06132, ν_{TZ} = 0.1807

The FE model consists of 30 elements along length, 30 elements along width and 4 elements along depth. The analytical results given in reference (Srinivas, 1970) are used to compare and validate FE results.

In this analysis, a study of through the thickness variation of stresses and out of plane deflection is performed for an orthotropic plate. Normalized values are plotted showing the comparison with the analytical solutions (Srinivas, 1970) in Figures 6 and 7. The FEA solution shows good agreement with the analytical solutions.

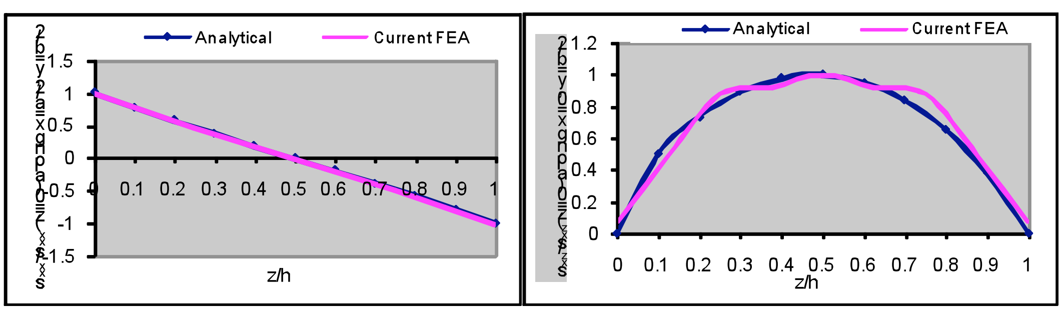

Figure 6. Through the thickness variation of normalized σ_{xx} and σ_{xz} stresses

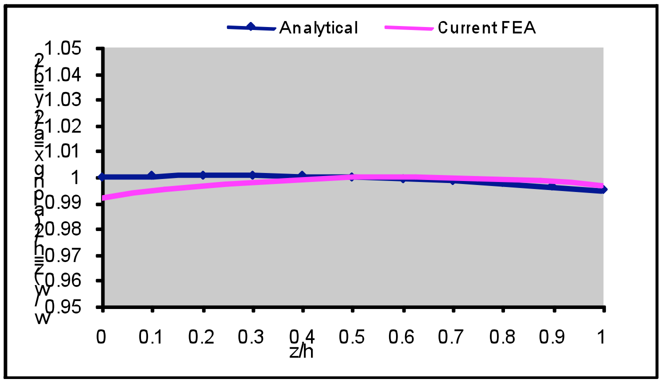

Figure 7. Through the thickness variation of normalized central deflection w

5. Study of stress concentration in notched plates under in-plane tension

A notched square plate with 50mm edge length is chosen for the study. It has a central hole of diameter 2.5mm. All the dimensions and axis system of the notched plate configurations are same as in Figure 3. The plate is subjected to uniform tension. In the current study the following four configurations have been studied.

Configuration I: Isotropic notched plate

Configuration II: Orthotropic plate with 0^0 fiber orientation

Configuration III: Orthotropic plate with 45^0 fiber orientation

Configuration IV: Orthotropic plate with 90^0 fiber orientation

The plate is modeled with S4 and C3D20 elements. The FE mesh used unstructured grid around the hole and transitioned to structured grid. The plate is modeled with the following boundary conditions assuming A, B, C, D are corner nodes of the plate

at corner A, displacements u=v=w=0; at corner B, displacements v=w=0; at corner C, displacement w=0

Uniformly distributed tensile load of 1 MPa is applied on edges AD and BC. Isotropic material properties are E = 210 GPa and ν = 0.3 and orthotropic plate properties are E_L = 137900 MPa, E_T = 10270 Mpa, G_{LT} = 2410 Mpa and ν_{LT} = 0.3.

All four plate configurations are studied and the results are compared with infinite plate solutions (William, 1985 and Barret, 1989). The loading angle is 0^0 and 90^0 from the fiber axis for configurations II, III and IV. Table 5 shows results for S4 and C3D20 elements.

Configuration	Element Type	Hole Boundary Tangential Stress (MPa) Angular location on hole circumference from X Axis			
		Abaqus Solution		Analytical Solution	
		θ = 0	θ = 90	θ = 0	θ = 90
I	S4	-0.981	2.988	-1.00	3.00
	C3D20	-1.079	3.088		

II	S4	-0.267	8.299	-0.273	8.997
	C3D20	-0.288	8.770		
III	S4	-0.795	2.034	-0.800	2.050
	C3D20	-0.817	2.051		
IV	S4	-3.351	3.166	-3.664	3.182
	C3D20	-3.679	3.273		

Table 5. Stress concentration factors for plate with a central hole subjected to uniform remote tension loading

C3D20 elements are able to accurately predict stress concentration factors along circular holes for both materials. In some cases, results provided by C3D20 elements are better than S4 elements even when the fineness of elements along the periphery of hole is higher in shell element model.

6. Analysis of laminated composite plates

A four ply symmetric square laminate under uniform lateral pressure of 1 MPa with simply supported boundary conditions has been analyzed. The following four configurations have been analyzed

Configuration I: Length 50mm, width 50mm, thickness 5mm & Stacking Sequence$[0/90]_s$

Configuration II: Length 50mm, width 50mm, thickness 5mm & Stacking Sequence$[45/-45]_s$

Configuration III: Length 100mm, width 200mm, thickness 5mm & Stacking Sequence $[45/-45]_s$
Configuration IV: Length 100mm, width 200mm, thickness 5mm & Stacking Sequence $[45/-45]_s$

All the dimensions and axis system of the plate configurations are same as in Figure 3. The plate is assumed to be simply supported with out of plane displacements w set to zero on all its four edges. Material properties used for configurations I, II and IV are

E_L = 210GPa, $E_T = E_Z$ = 8.4GPa, G_{LT}=G_{LZ}=4.2GPa, G_{TZ}=3.36GPa, $\nu_{LT} = \nu_{LZ} = \nu_{TZ}$ = 0.25

Material properties used for configurations III are

E_L = 210GPa, $E_T = E_Z$= 15.0GPa, G_{LT}=G_{LZ}=7.995GPa, G_{TZ}=4.845GPa,$\nu_{LT} = \nu_{LZ}$ = 0.3, ν_{TZ} = 0.55

The plate is analyzed using S4, C3D20 and layered C3D20 elements. Table 6 compares the FEA prediction of the central deflection (w) of various composite laminated plates with analytical solutions (Kabir, 1994). These predictions show very good agreement for cross ply symmetric laminate case and are close for angle ply symmetric laminates.

Configuration	Abaqus Solution			Analytical Solution
	Shell Element	Solid Element	Layered Solid Element	
I	0.057	0.06	0.06	0.057
II	0.042	0.055	0.055	0.042
III	0.457	0.52	0.52	0.448
IV	0.105	0.121	0.121	0.104

Table 6. Comparison of central deflection for various composite laminated plates subjected to lateral pressure

7. Study of edge effects on angle ply laminate under uniform axial strain

A symmetric angle ply laminate $[0/90]_s$ is analyzed to study the edge effects on stresses. Laminate configuration is taken from literature (Barboni, 1990) and the results are compared with the same. The ply is 0.125mm thick and is modeled using C3D20 elements. The laminate length (x), width (y) and thickness (z) are taken as 100mm, 8mm and 0.5mm respectively. The laminate axis system is same as in Figure 3. Laminate is subjected to uniform strain of one micron along length. Due to symmetry only half the dimensions are modeled in y & z directions and symmetry boundary conditions are applied at y=0 and z=0 planes. Each ply is modeled using two elements through the thickness and mesh is finer near the free edge. Ply material properties are

$E_L = 137.9$ GPa, $E_T = E_Z = 14.5$ GPa, $G_{LT} = G_{LZ} = G_{TZ} = 5.9$ GPa, $\nu_{LT} = \nu_{LZ} = \nu_{TZ} = 0.21$

Interlaminar normal stress is normalized with respect to the applied strain and is plotted along y in Figure 8. Edge effect can be seen near the free edge as the stresses peak near the free edge. The stress variation is very similar to the one predicted in literature (Barboni, 1990). In Figure 8, case A corresponds to M=2, K=1 and case B corresponds to M=4, K=3, where M and K are the number of terms in the series for displacement functions. C3D20 elements gave very good results for composite laminated plates and matched well with the analytical solutions. The layered solid elements will help in reducing the size of the problem drastically. The results obtained through layered solid elements are encouraging and can be used for global model analysis and preliminary design. The C3D20 elements predict the peaking of stresses near free edge. This will help us in implementing point stress and average stress failure criteria for composite laminates.

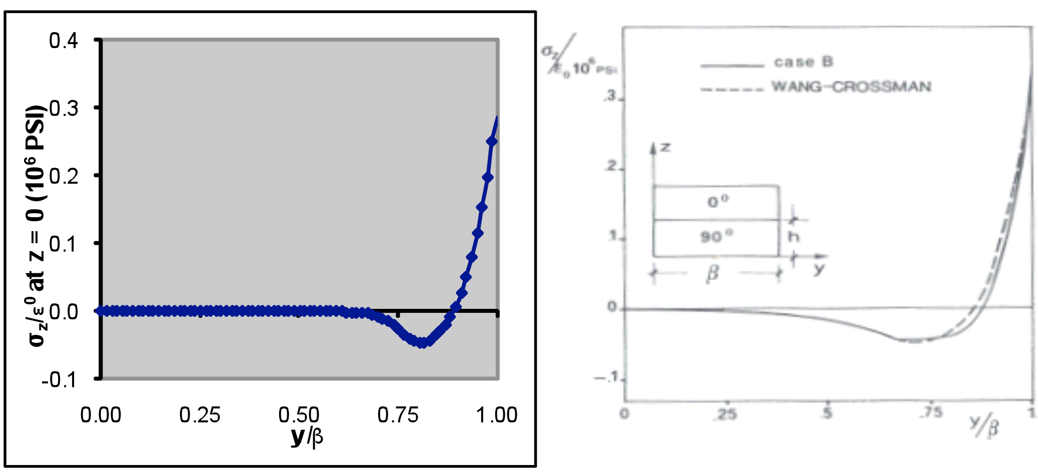

Present Analysis Barboni

Figure 8. Normal stress (σ_{zz}) plotted along y axis at z=0 for angle ply laminate under uniform axial strain

8. Analysis of advanced hybrid aircraft wing skin panel

A typical aircraft lower wing skin panel was analyzed to demonstrate the effectiveness of C3D20 elements in computation of 3D stress state in real life aircraft problems. The advanced hybrid stiffened panel considered in the study is similar to the one cited in the literature (Heinimann, 2007) . The details of the stiffened panel cross section of the wing skin and stringer and layup of the hybrid wing skin laminate is shown in Figure 9. GFRP layers are aligned along the stringers.

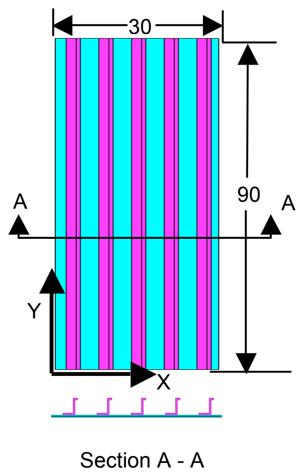

All dimensions are in inch

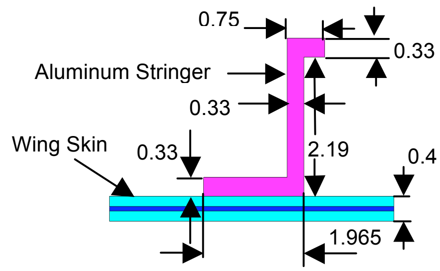

Layer Number	Layer Material	Thickness (inch)
1	Aluminum	0.1915
2	GFRP layer	0.005
3	Aluminum	0.016
4	GFRP layer	0.005
5	Aluminum	0.016
6	GFRP layer	0.005
7	Aluminum	0.1915

Wing skin lay up

Figure 9. Plan and cross section view of the wing panel

Aluminum E and ν are taken as 1.0E+07 psi and 0.3 respectively. Aluminum was modeled as elasto-plastic material and its True Stress - True Strain curve is shown in Figure 10:

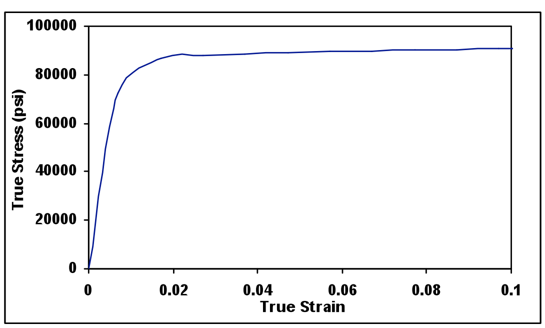

Figure 10. Aluminum true stress – true strain curve

The glass-fiber composite layer was modeled with the following material properties:

E_L = 7.186E6 psi, $E_T = E_Z$ = 7.5E5 psi, $G_{LT} = G_{TZ} = G_{ZT}$ = 2.85E+05 psi, $\upsilon_{LT} = \upsilon_{LZ} = \upsilon_{ZT}$ = 0.27

Global model was created using S4 elements. Edges of the panel as shown in Figure 9 have following boundary conditions:

u=w=0 along edges x= 0 & x= length; u=v=w=0 along edge y = 0; u=w=0, v= 0.36 inch along edge y = width

The panel is subjected to in-plane displacement of 0.36 inch along the width causing a nominal tensile strain of 0.004 and a normal pressure of 18 psi acting from outside of panel to inside (the inside of panel is the side on which stringers are attached).

Deflection and in-plane stress (σ_{xx} and σ_{yy}) patterns for the panel under the load are depicted in Figure 11. Maximum deflection is 0.367 inch at the centre of the panel.

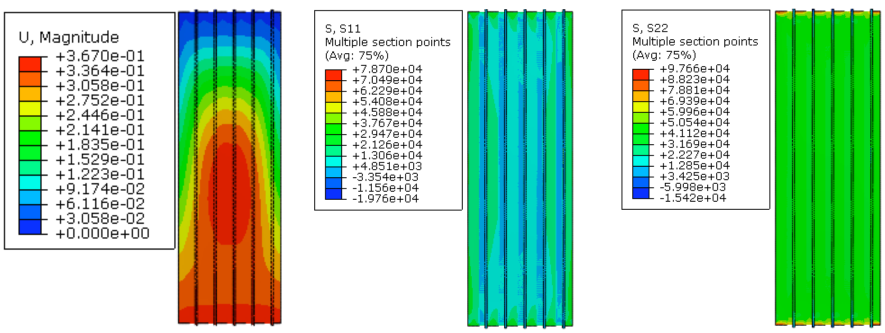

Displacements are in inch and stresses are in psi

Figure 11. Global Model: Deflection and in-plane stress contours

It is not possible to obtain out-of-plane stresses from the shell model. Out-of-plane stresses are not very important in thin sheet-metal components as most of the normal load is reacted by membrane in-plane stress. But in hybrid panels, out-of-plane stresses are very important as they may cause interlaminar failure. Solid elements are needed to predict out-of-plane stresses. But full finite element model of the panel with solid elements requires huge amount of computational time and resources for analysis. Thus in the current approach, global model is first analyzed with only shell elements. Then the identified critical region (local model) is extracted and modeled in detail with solid elements. Boundary node displacements from global simulation are applied as boundary conditions to the local model with appropriate interpolations. Thus the current global – local approach provides accurate insight to the 3-D stress field in the identified critical area.

8.1. Local Model

Local model was built solely with C3D20 elements based on the studies presented in previous sections. Nodal displacement on the boundary nodes of local model were obtained from the global model and applied to the local model. Global model has shell elements with six degrees of freedom at each node. Solid elements do not have rotational degrees of freedom. Hence nodal rotations from global model are converted to appropriate translational values. Interpolation is done to get the translation values for nodes which are not part of local model boundary in global model. All this is done by algorithm built-in in Abaqus. As in global model, pressure loading of 18 psi has been applied on the local model.

Local model was built from the global model considering the location where displacement is highest. This region is in the centre of the panel and is shown in Figure 12.

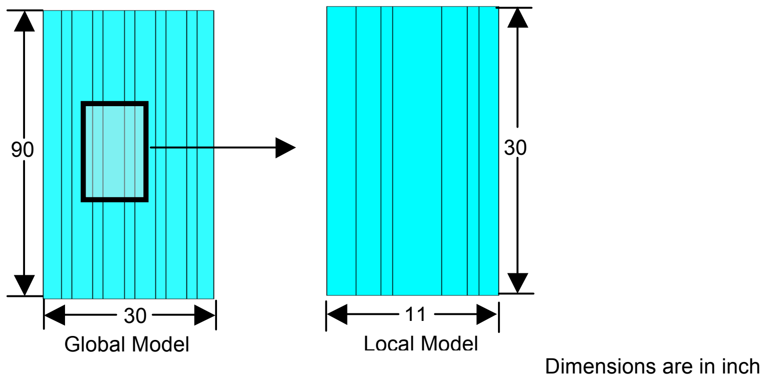

Figure 12: Global Model – Local Model

Deflection and in-plane stress patterns for the global and local models are depicted the Figure 13. Maximum deflection is 0.367 inch. This is exactly same as in global model. The contour patterns are also same in both the models. Hence it can be inferred that the interpolation of displacements from global to local model is working correctly.

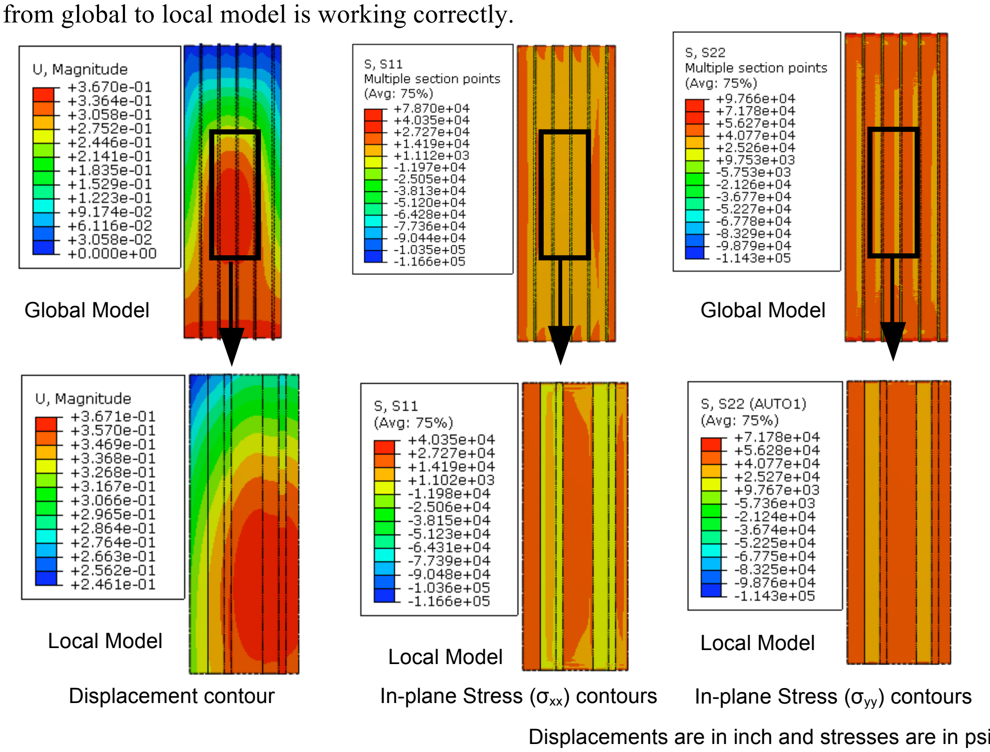

Figure 13. Global Model and Local Model comparisons

Figure 13 shows good correlation between the deflection and in-plane stress patterns and values in the global and local models. Out-of-plane stress (σ_{zz}, σ_{xz} and σ_{yz}) for local model are depicted in Figure 14.

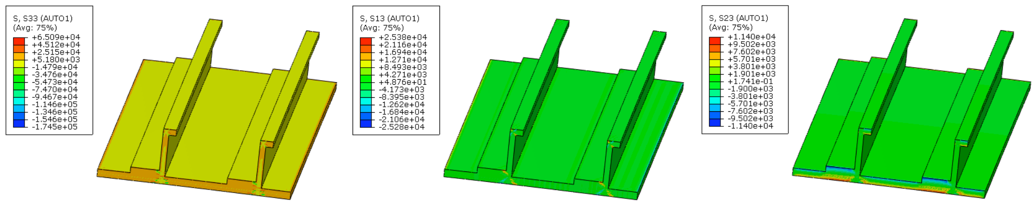

Figure 14. Local Model: Out-of-plane Stress contours

This study corroborates the importance of deploying global-local simulation strategy to simulate large panels wherein global shell models are used to generate component bulk results and local detailed solid models are used to perform detailed study of critical regions and to obtain point results useful to ascertain failure.

9. Conclusions

C3D20 elements have given very good results for isotropic, orthotropic and composite laminated plates. These elements are able to predict the both in plane and out of plane stresses as well as peaking of stresses near free edges very well. Stresses obtained from one/two elements through the thickness have predicted displacements and stresses very close to the available solutions in the literature. C3D20 elements are able to accurately predict stress concentration factors along circular holes in isotropic/orthotropic plates under in-plane loading. In some cases, results provided by C3D20 elements are better than S4 elements even when the fineness of elements along the periphery of hole is more in shell element model. C3D20 elements have computed accurate interlaminar stresses in orthotropic plates under transverse load. We propose C3D20 elements to be used for the analysis as failure using stress components has to be implemented at integration points of the elements. Global local analysis approach for hybrid stiffened panel has been demonstrated for real life large size problem. For detailed local analysis, C3D20 elements are suggested with at least one element per layer. Also it is suggested that very fine mesh is used near the free edges (element size less than thickness of the laminate) to capture the free edge effects and to apply failure theories accurately. C3D20 element has shown to be high performing element and is strongly recommended for the analysis of hybrid laminated structures. Abaqus is recommended for analysis of hybrid laminated structures for its strong nonlinear analysis and contact modeling capabilities and provision for writing user subroutines for failure analysis.

References

1. Barboni R, Gaudenzi P, Carlini S, “A Three-Dimensional Analysis of Edge Effects in Composite Laminates with Circular Holes”, Composite Structures 1990, 15:115-136.
2. Barret NB, “Stress Concentration around holes in Composite Plates”, MSc Research Thesis, Cambridge Institute of Technology, 1989.

3. Bucci RJ, “Advanced Metallic & Hybrid Structural Concepts”, In: USAF Structural Integrity Program Conference (ASIP 2006), San Antonio, Texas, November 29, 2006.
4. Ganapathy S, “Quasi static non-linear finite element analysis for predicting damage in plain/stiffened laminated composite plates/shell panels subjected to low-velocity impact”, Ph.D. thesis, Indian Institute of Science, Bangalore, India, March 1998.
5. Ganapathy S, Rao KP, “Failure analysis of laminated composite cylindrical/spherical shell panels subjected to low velocity impact”, Computers and Structures 1998; 68:627-641
6. Heinimann MB, Bucci RJ, Garratt MD, Kulak M, “Improving Damage Tolerance of Aircraft Structures through the use of Selective reinforcement”, In: Proceedings International Committee on Aeronautical Fatigue (ICAF), Hamburg, Germany 2005.
7. Heinimann MB, Bucci RJ, Kulak M, Shoup FA, Hinrichsen J, Roebroeks GHJJ, Hooijmeijer P A,” Advanced Hybrid Structural Concepts for Care-Free Structures: Experimental Validation and Path Forward”, In: ASIP Conference, Palm Springs, California, 2007.
8. Heinimann MB, Kulak M, Bucci RJ, James M, Wilson G, Brockenbrough J, Zonker H, Sklyut H, “Validation of Advanced Metallic Hybrid Concept with Improved Damage Tolerance Capabilities for next generation lower wing and fuselage applications”, 24th ICAF Symposium, Naples 2007
9. James MG, Timoshenko S P, “Mechanics of Materials”, 2nd Edition, PWS Publisher, 1984.
10. Kabir HRH,” Analysis of a simply supported plate with symmetric angle-ply laminations”, Computers and Structures 1994; 51(3):299-307.
11. Kulak M, Bucci RJ, Heinimann MB, Bodily B, Spinella DJ, DiCocco F, “Lightweight Aluminum Wing Structures (LAWS) – Advanced Structural Technologies, NASA Contract Number: NNL04AA35C – Phase 1 Final Report”, National Aeronautics & Space Administration 2004.
12. Srinivas S, “Three-Dimensional analysis of some plates and laminates and a study of thickness effects”, Ph.D. Thesis, Indian Institute of Science, Bangalore, India, 1970.
13. Timoshenko SP, Krieger SW, “Theory of plates and shells”, McGraw-Hill International Editions, 1959.
14. William LK, “Stress Concentration around a Small Circular Hole In The HiMAT Composite Plate”, NASA Technical Memorandum 86038, December, 1985.